Journal of Structural Geology, Vol. 11, No. 7, pp. 873 to 877, 1989
Printed in Great Britain

0191-8141/89 $03.00 + 0.00
Pergamon Press plc

High-angle reverse faulting in northern New Brunswick, Canada, and its implications for fluid pressure levels

RICHARD H. SIBSON

Department of Geological Sciences, University of California, Santa Barbara, CA 93106, U.S.A.

(*Received 7 January* 1989; *accepted in revised form* 3 *April* 1989)

Abstract—The 1982 Miramichi earthquake sequence in northern New Brunswick included four shocks in the magnitude range, 5.7 > $\mathbf{m}_b$ > 5.0, and extensive aftershock activity. Rupturing occurred within granitic terrain on a pair of NNE–SSW-striking, opposite-facing, high-angle reverse faults which converge at the mainshock focal depth of ~7 km. It seems probable that the earthquake sequence involved the reactivation under horizontal compression of an existing set of steep normal faults, perhaps derived from Mesozoic rifting of the Atlantic continental margin. The symmetry of the V-shaped profile of faults in WNW–ESE section suggests that the maximum principal compressive stress (σ_1) during reactivation was subhorizontal and the least principal stress (σ_3) was subvertical, so that the reactivation angle between σ_1 and the faults corresponded to the 50–65° dip of the faults. Stress analysis of the conditions for frictional reactivation of existing cohesionless faults shows that pore-fluid pressures approaching or exceeding lithostatic values are required for reshear at such high reactivation angles, with the implication that the earthquake sequence was triggered by locally elevated fluid pressure. While the source and composition of the inferred high pressure fluids are uncertain, a mixed H_2O–CO_2 fluid of mantle origin seems most likely.

INTRODUCTION

IN COMPARISON with interplate earthquakes, where the cycles of strain accumulation leading to elastic rebound along major fault systems are driven by relative plate motion and can be directly observed, the processes causing intraplate seismic failure in continental interiors are not well understood. Over broad regions of Australia or eastern North America, focal mechanisms obtained from intraplate earthquakes are either strike-slip or reverse dip-slip, indicating a state of fairly uniform horizontal compressive stress (Sykes & Sbar 1973, Zoback & Zoback 1980, Fredrich *et al.* 1988). This suggests that the upper crust in such regions is acting as a compressional stress guide. However the details of what triggers seismogenic failure at a particular place and time are generally unclear.

The 1982 Miramichi earthquake sequence in northern New Brunswick (Fig. 1) is of particular significance in this regard because its well constrained rupture geometry, involving symmetrical high-angle reverse faulting on opposite-dipping planes, allows a simple rock mechanics analysis of the stress and fluid pressure conditions at failure. An important inference from the analysis is that at least some intraplate earthquakes are triggered by the local elevation of pore fluid pressures to approximately lithospheric values.

1982 MIRAMICHI EARTHQUAKE SEQUENCE

The Miramichi sequence began on the morning of 9 January 1982 with an $\mathbf{m}_b$ 5.7 earthquake which nucleated at a depth of ~7 km (Wetmiller *et al.* 1984). This mainshock was followed by an extensive series of aftershocks (>800 detected) which included an $\mathbf{m}_b$ 5.1 aftershock some 3½ hours after the main event, an $\mathbf{m}_b$ 5.4 event on 11 January and an $\mathbf{m}_b$ 5.0 event on 31 March. High precision location of the aftershock foci showed them to be grouped about two NNE–SSW-striking planes, dipping steeply in opposite directions and converging at the mainshock focal depth of ~7 km to define a V-shaped profile in WNW–ESE section. Focal mechanism studies of the four principal ruptures, coupled with waveform modelling, showed them to result from reverse faulting on the two oppositely dipping planes as shown in Fig. 2. From teleseismic analysis, Choy *et al.* (1983) calculated that the slip vector for the main rupture raked 70°NNE in a plane dipping 65°WNW. Estimates for the dips of the four individual rupture planes ranged from 50° to 65°, though there is some indication that the planes steepen as they approach the surface (Wetmiller *et al.* 1984, Basham & Kind 1986). The earthquake sequence thus involved almost pure reverse faulting on steep, opposite-dipping planes.

The epicentral distribution of the earthquakes occurred largely within the surface outcrop of a Devonian granitic pluton intruding a thick sequence of earlier deformed granitoids and Ordovician metasediments (Fig. 1). On the basis of gravity data, the earthquakes are believed to have occurred almost entirely within the body of the pluton (Basham & Adams 1984). Surface mapping failed to find a definite surface rupture associated with the earthquake sequence, though a superficial 'thrust pop-up' appeared more-or-less along the projected outcrop of the W-dipping plane (Wetmiller *et al.* 1984). Nor is the NNE–SSW strike of the main rupture planes matched by any obvious structural trends visible at the surface, though NE–SW diabase dikes of late Triassic to early Jurassic age,

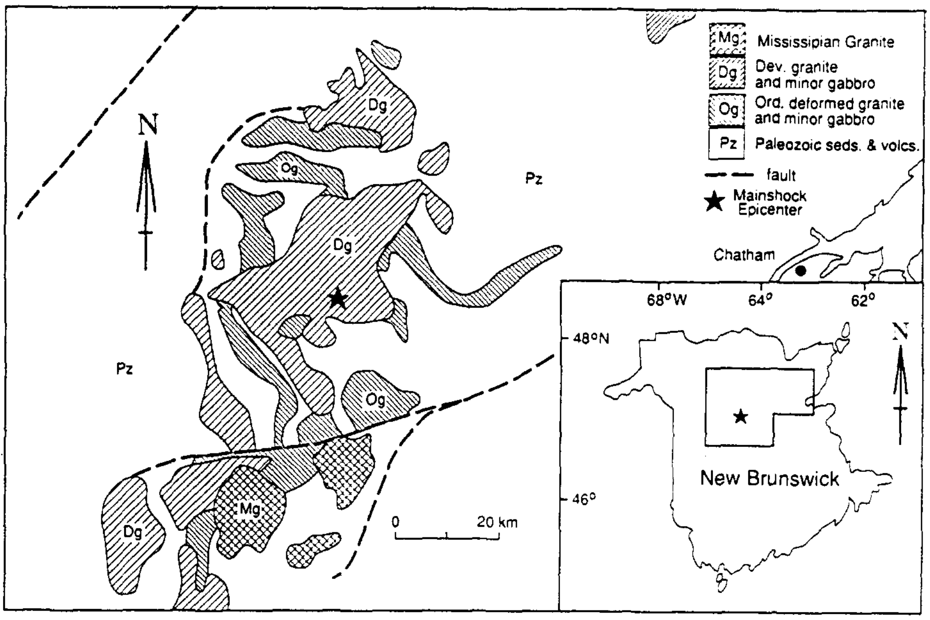

Fig. 1. Location map for the 1982 Miramichi earthquake sequence in northern New Brunswick, Canada (after Ferguson & Fyffe 1985).

perhaps intruded during the initial rifting of the present Atlantic Ocean, occur to the east (Ferguson & Fyffe 1985). From microstructural analysis, Mawer & Williams (1985) noted that the granitic body is pervaded by multiple generations of microfractures which they attributed to periodic, fluid-assisted fracturing.

FAILURE MECHANICS

The geometry of the Miramichi earthquake sequence is sufficiently well-constrained from seismology to allow a simple rock mechanics analysis of the failure conditions at the mainshock focal depth of ~7 km. For the purpose of the analysis the slight strike-slip component is neglected, and pure high-angle reverse faulting is taken to have occurred on the opposite-dipping planes. This approximation allows us to neglect the effect of the intermediate principal compressive stress (σ_2), a not unreasonable assumption given the high rake value estimated for the slip vector. An important inference from the upright V-symmetry of the two sets of rupture planes in WNW–ESE cross-section is that the principal stress trajectories responsible for the reverse faulting must lie either perpendicular or parallel to the earth's surface, in accordance with surface boundary conditions (Anderson 1951). For the observed senses of shear, the least principal compressive stress (σ_3) must therefore be subvertical, and the maximum compressive stress (σ_1) must lie subhorizontal oriented WNW–ESE as illustrated in Fig. 3.

The dotted lines in Fig. 3 show the orientation of *Andersonian* thrust faults which would be expected to form in homogeneous, isotropic rock under this stress field. This emphasizes that the Miramichi earthquake sequence probably involved the preferential reactivation of steep pre-existing faults, perhaps normal faults formed during an earlier episode of extension as inferred elsewhere along the Atlantic seaboard (Sykes 1978). It is also apparent from Fig. 3 that the angle of reactivation (θ_r) between σ_1 and the faults corresponds to their estimated dip values, so that $50° < \theta_r < 65°$.

Conditions for frictional reactivation

In a triaxial stress state (effective principal compressive stresses, $\sigma_1' = (\sigma_1 - P_f) > \sigma_2' = (\sigma_2 - P_f) >$

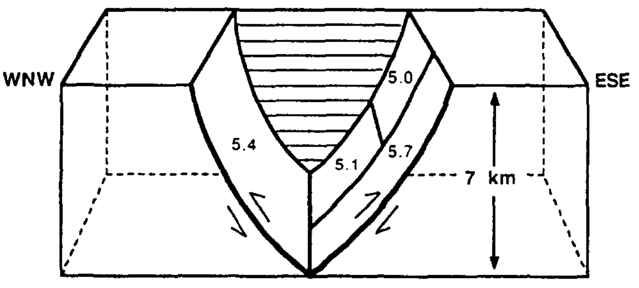

Fig. 2. Block diagram, viewed looking NNE, of the V-shaped pattern defined by the main rupture planes in the Miramichi earthquake sequence (after Wetmiller *et al.* 1984).

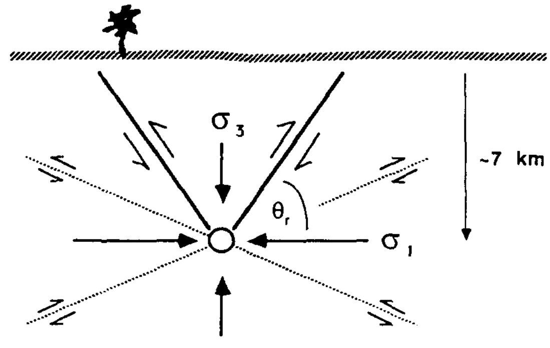

Fig. 3. Schematic WNW–ESE section through the Miramichi ruptures showing the reactivation angle, θ_r, in relation to the inferred stress trajectories. Light dotted lines delineate expected orientation of thrusts formed by shear failure of intact rock in the same stress field.

$\sigma_3' = (\sigma_3 - P_f)$, where P_f is the fluid pressure), the criterion for frictional reactivation of an existing cohesionless fault plane may be approximated by Amonton's Law,

$$\tau = \mu_s \sigma_n' = \mu_s(\sigma_n - P_f), \qquad (1)$$

where τ and σ_n are, respectively, the resolved shear and normal stresses on the plane and μ_s is the static coefficient of rock friction. A μ_s value of 0.75 gives a good approximation to Byerlee's (1978) general laws of rock friction (see Sibson 1983). Note that for this and comparable frictional criteria, it is apparent that shear failure could be induced by increasing τ, by decreasing σ_n or by increasing P_f.

For the two-dimensional situation in Fig. 3, this condition for reactivation may be rewritten (Sibson 1985) as,

$$(\sigma_1'/\sigma_3') = (1 + \mu_s \cot\theta_r)/(1 - \mu_s \tan\theta_r) \qquad (2)$$

or

$$(\sigma_1 - \sigma_3) = \mu_s[(\tan\theta_r + \cot\theta_r)/(1 - \mu_s \tan\theta_r)]\sigma_3'. \qquad (3)$$

At a depth, z, the effective vertical stress is,

$$\sigma_v' = (\sigma_v - P_f) = \rho\, g\, z(1 - \lambda_v), \qquad (4)$$

where ρ is the average density of the rock overburden, g is the gravitational acceleration, and the pore-fluid factor, $\lambda_v = (P_f/\rho\, g\, z)$, the ratio of fluid to overburden pressure. Thus for the illustrated stress field where the vertical stress, $\sigma_v' = \sigma_3'$, equations (3) and (4) may be combined to yield,

$$(\sigma_1 - \sigma_3) = \mu_s[(\tan\theta_r + \cot\theta_r)/(1 - \mu_s \tan\theta_r)]\rho g z(1 - \lambda_v) \qquad (5)$$

an expression giving the differential stress required for frictional reactivation at a depth, z, for particular values of ρ, μ_s, θ_r, and λ_v.

The curves in Fig. 4 plot the differential stress required for frictional reactivation at a depth of 7 km (corresponding to the focal depth of the Miramichi mainshock) vs the reactivation angle, θ_r, for different values of the pore-fluid factor, λ_v, when $\mu_s = 0.75$ and $\rho = 2650$ kg m^{-3}, a representative density for the granitic pluton (Burke & Chandra 1983). The shaded area defines the range of likely reactivation angles for the Miramichi ruptures. For any particular value of λ_v, the differential stress required for reactivation has a minimum value at the optimum angle for reactivation given by $\theta_r^* = 0.5 \tan^{-1}(1/\mu_s)$. When $\mu_s = 0.75$, $\theta_r^* \approx 27°$. An important point is that for $\theta_r > 2\theta_r^*$, a necessary condition for reactivation is that $P_f > \sigma_3$, or $\lambda_v > 1$ in this stress configuration (Sibson 1985).

In consideration of these curves, bear in mind first that despite uncertainties in our knowledge of the average differential stress level within the earth's crust and upper mantle, an upper bound of a few hundred megapascals is generally considered probable, even in cold intraplate regions (see Hanks & Raleigh 1980). In such regions, the background state of fluid pressure within the upper crust might generally be expected to be hydrostatic ($\lambda_v \sim 0.4$), corresponding to a fracture network inter-

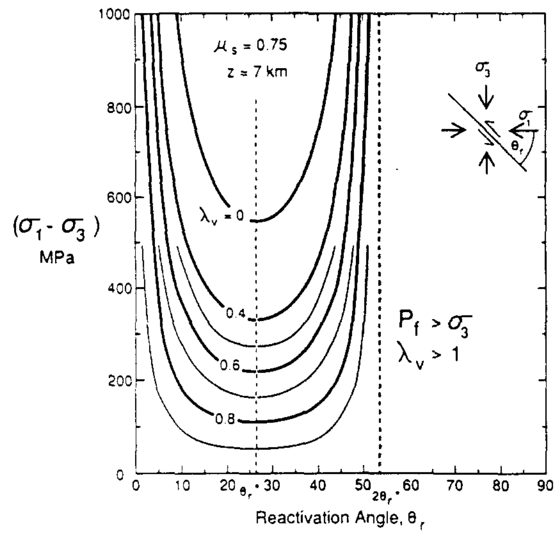

Fig. 4. Plot of the differential stress ($\sigma_1 - \sigma_3$) required for frictional reactivation of cohesionless faults at 7 km depth vs the reactivation angle, θ_r, for different values of the pore-fluid factor, λ_v, and for an average crustal density, $\rho = 2650$ kg m^{-3}. The hydrostatic fluid pressure condition is approximated by the $\lambda_v = 0.4$ curve. Shaded area represents the range of reactivation angles for the Miramichi ruptures. The field $\lambda_v > 1$ lies to the right of the dashed line at $\theta_r = 2\theta_r^*$.

connected through to the surface. Note then, that even at the optimum reactivation angle under hydrostatic fluid pressures, the differential stress required for frictional reactivation at 7 km depth is nearly 400 MPa. As θ_r increases towards the Miramichi range of values, the required differential stress becomes improbably large. It is only with λ_v values approaching or exceeding unity that reactivation at these angles becomes possible under feasible stress levels.

The condition $\lambda_v > 1$ can only be achieved when $P_f > \sigma_v = \sigma_3$, and the extent to which this can occur is limited by the tensile strength of the rock, T, since hydraulic extension fracturing will occur when the condition,

$$P_f = \sigma_3 + T \qquad (6)$$

is met. If, for example, we take $T = 10$ MPa as a likely upper limit (Etheridge 1983), the maximum λ_v sustainable at a depth of 7 km is ~1.05. For this λ_v value and for the same friction coefficient used above, equation (5) then allows us to calculate that reactivation of an existing fault oriented at 65° to σ_1 would occur under a differential stress of only 30 MPa.

Reactivation vs intact shear failure

An alternative analysis considers the conditions that must be met for reactivation of an unfavorably oriented fault to occur in preference to shear failure of the surrounding intact rock. The general Coulomb criterion for shear failure of material under compression,

$$\tau = C + \mu_i \sigma_n' = C + \mu_i(\sigma_n - P_f), \qquad (7)$$

where C and μ_i are, respectively, the cohesive strength and internal friction of the material, may be rewritten in terms of the effective principal stresses as,

$$\sigma_1' = \sigma_0 + K\sigma_3' \quad (8)$$

or

$$(\sigma_1 - \sigma_3) = \sigma_0 + (K - 1)\sigma_3', \quad (9)$$

where σ_0 is the uniaxial compressive strength of the material, and $K = (\sqrt{1 + \mu_i^2} + \mu_i)^2$. From equations (3) and (9), the boundary condition where reactivation and intact shear failure occur at the same differential stress level is given by,

$$\mu_s[(\tan\theta_r + \cot\theta_r)/(1 - \mu_s\tan\theta_r)] = (\sigma_0/\sigma_v') + (K - 1). \quad (10)$$

This bounding condition is illustrated in Fig. 5, where the Mohr circle representing a particular differential stress state is tangential to the intact failure envelope while satisfying the condition for reactivation of a cohesionless fault oriented at an angle θ_r to σ_1. For simplicity, it is assumed that $\mu_i = \mu_s = 0.75$, a reasonable assumption given that $0.5 < \mu_i < 1.0$ for almost all rocks (Jaeger & Cook 1979).

Using this relationship, the fields of reshear and intact shear failure are defined on a plot of λ_v vs the reactivation angle, θ_r (Fig. 6), computed from equation (10) for a depth of 7 km with $\sigma_0 = 100$ MPa. This value of uniaxial compressive strength, about half that found in short-term laboratory tests (Jaeger & Cook 1979), has been adopted as a reasonable estimate for the long-term strength of granitic rock (Price 1966). It is readily apparent from Fig. 6 that, for the Miramichi range of reactivation angles, reshear will occur in preference to intact shear failure only with λ_v values approaching or slightly exceeding unity.

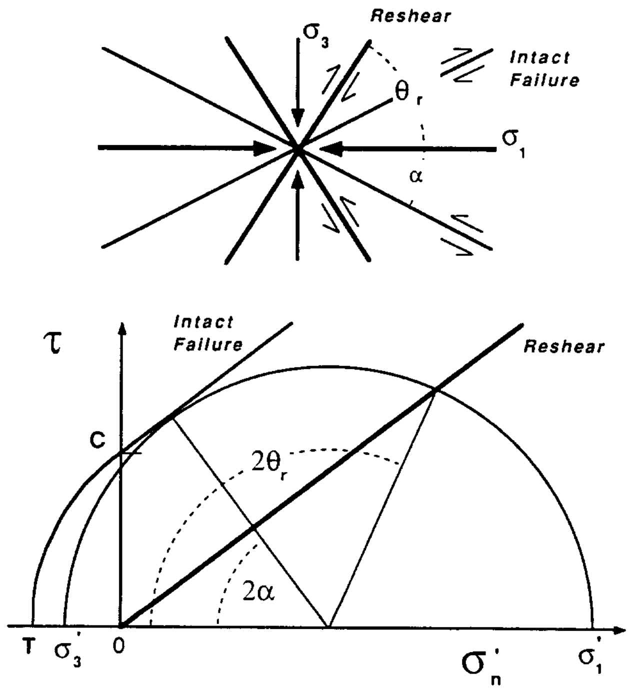

Fig. 5. Mohr diagram of shear stress, τ, vs effective normal stress, σ_n', showing the failure conditions for frictional reactivation (reshear) of a cohesionless fault and for failure of intact rock with $\mu_i = \mu_s = 0.75$. Illustrated stress state allows simultaneous intact shear failure, forming faults at an angle α to σ_1, and reshear of a fault oriented at an angle θ_r to σ_1.

With regard to both the above analyses, it might be argued that the problem of reactivating unfavorably oriented faults would be less severe if the friction coefficient were lower. On the basis of hydrofracture stress measurements in the vicinity of active faults, Zoback & Healy (1984) generally inferred friction coefficients in the range 0.6–1.0, comparable to Byerlee's (1978) experimental results, but estimated a value as low as 0.4 in the vicinity of the San Andreas fault. This last value would allow reactivation at θ_r angles up to ~70° without the need for the condition $P_f > \sigma_3$. However, in intraplate regions where the recurrence interval between successive earthquakes is likely to be very large and the total fault displacement is probably small, Byerlee-type values for rock friction would seem to be more appropriate. It should be noted, moreover, that: (i) the frictional strength of rock surfaces in contact generally increases with time (Dieterich 1978); and (ii) some cementation of discontinuities may occur with time through hydrothermal deposition (Angevine *et al.* 1982), imparting cohesive strength to existing faults. This latter strengthening effect, in particular, may reduce the strength differential between the fault and the country rock, so that the requirement for abnormal fluid pressure levels to reactivate faults that are unfavorably oriented becomes even greater.

Analogy with mesothermal gold–quartz lodes

Direct evidence that supralithostatic fluid pressures are associated with steep reverse faulting comes from gold–quartz vein systems hosted in ancient high-angle reverse or reverse-oblique shear zones, exhumed from depths equivalent to the foci of moderate-to-large crustal earthquakes (Sibson *et al.* 1988). Typically, the hosting fault zones exhibit mixed 'brittle–ductile'

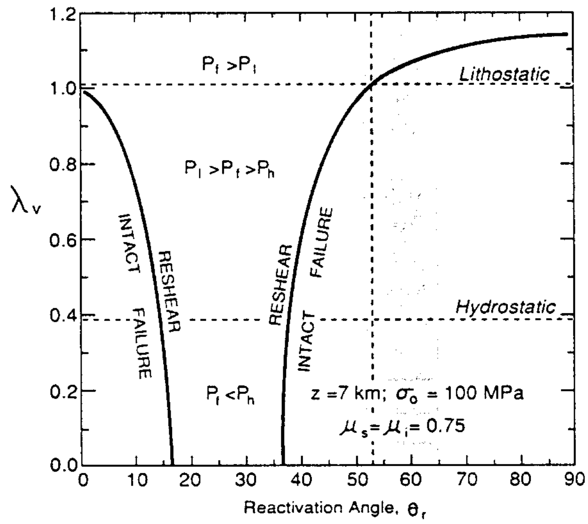

Fig. 6. Graph of the pore-fluid factor, λ_v, vs the reactivation angle, θ_r, defining fields of reshear and intact shear failure at a depth of 7 km for material with a uniaxial compressive strength of 100 MPa and $\mu_i = \mu_s = 0.75$. Shaded area represents the range of reactivation angles for the Miramichi ruptures, P_l and P_h represent lithostatic and hydrostatic levels of fluid pressure, respectively.

character and are comparatively small displacement structures (<100 m or so). The composite vein systems, with textures recording histories of incremental deposition, are made up of fault-veins within the steeply-dipping shear zones (attributed to episodes of post-failure discharge) and associated subhorizontal extension veins. These latter demonstrate unequivocably that the condition, $P_f > \sigma_v = \sigma_3$, was met intermittently during fault activity. The ancient structures therefore present a remarkable analog to the nucleation sites of modern high-angle reverse ruptures, such as those in the Miramichi area.

DISCUSSION

Despite the approximations in the analysis, it seems clear that the Miramichi earthquake sequence must have been triggered by fluid pressure levels locally elevated to approach or slightly exceed the lithostatic load. Nor is this just an isolated case of high-angle reverse faulting in eastern North America. Several other examples are known, for example the $\mathbf{m}_b$ 5.2 Goodnow, New York, earthquake of 1983 (Seeber *et al.* 1984). Given that these high-angle ruptures are triggered by elevated fluid pressures, it seems quite probable that other intraplate events involving different modes of faulting may similarly by fluid-induced. An obvious comparison may be made with earthquakes induced by the impounding of large reservoirs in plate interiors (Talwani & Acree 1985). The case for fluid triggering of intraplate seismicity has recently been advanced by Costain *et al.* (1987), but their *hydroseismicity* hypothesis involves comparatively low amplitude fluctuations in fluid pressure at close to hydrostatic values. Evidence presented here for faulting induced by near-lithostatic fluid pressures is more in accord with the ideas of Gold & Soter (1985), who attribute much seismogenic failure to the upwards migration of high-pressure fluids from the deep earth.

The outstanding question, of course, is the origin and nature of the inferred high-pressure fluids. Clues come from two separate sources. First, there is the remarkable global correlation between present-day seismic belts and the distribution of CO_2-rich springs noted by Irwin & Barnes (1980). This association extends even to areas of intraplate seismicity such as the Saint Lawrence Valley in eastern Canada. Isotopic evidence suggests that much of the carbon dioxide is derived from the mantle. Second, fluid inclusion studies of the mesothermal gold–quartz vein systems described above suggest that a low-salinity fluid of mixed H_2O–CO_2 composition was responsible for the mineralization (Robert & Kelly 1987). The high-pressure fluids thus seem most likely to be of mixed H_2O–CO_2 composition and to have originated in the mantle.

Acknowledgements—I thank Jack Boatwright and Noel Barstow for alerting me to the peculiar characteristics of intraplate earthquakes in eastern North America. This work was supported by National Science Foundation Grant EAR86-07445 and U.S. Geological Survey Grant 14-08-0001-G1331.

REFERENCES

Anderson, E. M. 1951. *The Dynamics of Faulting* (2nd edn). Oliver & Boyd, Edinburgh.

Angevine, C. L., Turcotte, D. L. & Furnish, M. D. 1982. Pressure solution lithification as a mechanism for the stick–slip behavior of faults. *Tectonics* **1**, 151–160.

Basham, P. W. & Adams, J. 1984. The Miramichi, New Brunswick earthquakes: near-surface thrust faulting in the northern Appalachians. *Geosci. Can.* **11**, 115–121.

Basham, P. W. & Kind, R. 1986. GRF broad-band array analysis of the 1982 Miramichi, New Brunswick earthquake sequence. *J. Geophys.* **60**, 120–128.

Burke, K. B. S. & Chandra, J. J. 1983. Gravity survey of the epicentral area of the main sequence of the Miramichi earthquakes. New Brunswick Department of Natural Resources, Mineral Resources Division, Open-File Report **83-3**.

Byerlee, J. D. 1978. Friction of rocks. *Pure & Appl. Geophys.* **116**, 615–626.

Choy, G. L., Boatwright, J., Dewey, J. W. & Sipkin, S. A. 1983. A teleseismic analysis of the New Brunswick earthquake of January 9, 1982. *J. geophys. Res.* **88**, 2199–2212.

Costain, J. K., Bollinger, G. A. & Speer, J. A. 1987. Hydroseismicity: a hypothesis for the role of water in the generation of intraplate seismicity. *Seismol. Res. Lett.* **58**, 41–63.

Dieterich, J. H. 1978. Time-dependent friction and the mechanics of stick-slip. *Pure & Appl. Geophys.* **116**, 790–806.

Etheridge, M. A. 1983. Differential stress magnitudes during regional deformation and metamorphism—upper bound imposed by tensile fracturing. *Geology* **11**, 231–234.

Ferguson, L. & Fyffe, L. R. 1985. Geological highway map of New Brunswick and Prince Edward Island. *Spec. Publ. Atlantic Geol. Soc.* 2.

Fredrich, J., McCaffrey, R. & Denham, D. 1988. Source parameters of seven large Australian earthquakes determined by body waveform inversion. *Geophys. J. R. astr. Soc.* **95**, 1–13.

Gold, T. & Soter, S. 1985. Fluid ascent through the solid lithosphere and its relation to earthquakes. *Pure & Appl. Geophys.* **122**, 492–530.

Hanks, T. C. & Raleigh, C. B. 1980. The conference on magnitude of deviatoric stresses in the earth's crust and uppermost mantle. *J. geophys. Res.* **85**, 6083–6085.

Irwin, W. P. & Barnes, I. 1980. Tectonic relations of carbon dioxide discharges and earthquakes. *J. geophys. Res.* **85**, 3115–3121.

Jaeger, J. C. & Cook, N. G. W. 1979. *Fundamentals of Rock Mechanics* (3rd edn). Chapman & Hall, London.

Mawer, C. K. & Williams, P. F. 1985. Crystalline rocks as possible paleoseismic indicators. *Geology* **13**, 100–102.

Price, N. J. 1966. *Fault and Joint Development in Brittle and Semi-brittle Rock.* Pergamon Press, Oxford.

Robert, F. & Kelly, W. C. 1987. Ore-forming fluids in Archean gold-bearing quartz veins at the Sigma Mine, Abitibi greenstone belt, Quebec, Canada. *Econ. Geol.* **82**, 56–74.

Seeber, L. E., Cranswick, E., Armbruster, J. & Barstow, N. 1984. The October 1983 Goodnow N.Y. aftershock sequence: regional seismicity and structural features in the Adirondacks. *EOS Trans. Am. Geophys. Un.* **65**, 240.

Sibson, R. H. 1983. Continental fault structure and the shallow earthquake source. *J. geol. Soc. Lond.* **140**, 741–767.

Sibson, R. H. 1985. A note on fault reactivation. *J. Struct. Geol.* **7**, 751–754.

Sibson, R. H., Robert, F. & Poulsen, K. H. 1988. High-angle reverse faults, fluid-pressure cycling, and mesothermal gold–quartz deposits. *Geology* **16**, 551–555.

Sykes, L. R. 1978. Intraplate seismicity, reactivation of preexisting zones of weakness, alkaline magmatism, and other tectonism post-dating continental fragmentation. *Rev. Geophys.* **16**, 621–688.

Sykes, L. R. & Sbar, M. L. 1973. Intraplate earthquakes, lithospheric stresses and the driving mechanism of plate tectonics. *Nature* **245**, 298–302.

Talwani, P. & Acree, S. 1985. Pore pressure diffusion and the mechanism of reservoir-induced seismicity. *Pure & Appl. Geophys.* **122**, 947–965.

Wetmiller, R. J., Adams, J., Anglin, F. M., Hasegawa, H. S. & Stevens, A. E. 1984. Aftershock sequences of the 1982 Miramichi, New Brunswick, earthquakes. *Bull. seism. Soc. Am.* **74**, 621–653.

Zoback, M. D. & Healy, J. H. 1984. Friction, faulting, and *in situ* stress. *Ann. Geophys.* **2**, 689–698.

Zoback, M. L. & Zoback, M. 1980. State of stress in the conterminous United States. *J. geophys. Res.* **85**, 6113–6156.